

# Pro-atherogenic activation of A7r5 cells induced by the oxLDL/ $\beta_2$ GPI/anti- $\beta_2$ GPI complex

TING WANG\*, HANG OUYANG\*, HONG ZHOU, LONGFEI XIA, XIAOYAN WANG and TING WANG

Jiangsu Key Laboratory of Medicine Science and Laboratory Medicine, School of Medicine, Jiangsu University, Zhenjiang, Jiangsu 212013, P.R. China

Received March 15, 2018; Accepted July 30, 2018

DOI: 10.3892/ijmm.2018.3805

**Abstract.** A previous study has revealed that oxidized low-density lipoprotein (oxLDL)/ $\beta_2$ -glycoprotein I ( $\beta_2$ GPI)/anti- $\beta_2$ -glycoprotein I (anti- $\beta_2$ GPI), an immune complex, is able to activate the Toll-like receptor 4 (TLR4)/nuclear factor  $\kappa$ B (NF- $\kappa$ B) inflammatory signaling pathway in macrophages, and consequently enhance foam cell formation and the secretion of prothrombin activators. However, the effects of the oxLDL/ $\beta_2$ GPI/anti- $\beta_2$ GPI complex on vascular smooth muscle cells have yet to be investigated. The present study investigated whether the oxLDL/ $\beta_2$ GPI/anti- $\beta_2$ GPI complex was able to reinforce the pro-atherogenic activities of a rat thoracic aorta smooth muscle cell line (A7r5) and examined the underlying molecular mechanisms. The results revealed that the oxLDL/ $\beta_2$ GPI/anti- $\beta_2$ GPI complex treatment significantly ( $P < 0.05$  vs. the media, oxLDL, oxLDL/ $\beta_2$ GPI and  $\beta_2$ GPI/anti- $\beta_2$ GPI groups) enhanced the pro-atherogenic activation of A7r5 cells, including intracellular lipid loading, Acyl-coenzyme A cholesterol

acyltransferase mRNA expression, migration, matrix metalloproteinase-9 and monocyte chemoattractant protein 1 secretion, all via TLR4. In addition, the expression of TLR4 and the phosphorylation of NF- $\kappa$ B p65, p38 and ERK1/2 were also upregulated in oxLDL/ $\beta_2$ GPI/anti- $\beta_2$ GPI complex-treated A7r5 cells. Pre-treatment with TAK-242, a TLR4 inhibitor, was able to partly attenuate the oxLDL/ $\beta_2$ GPI/anti- $\beta_2$ GPI complex-induced phosphorylation of NF- $\kappa$ B p65; however, it had no effect on the phosphorylation of extracellular regulated kinase 1/2 (ERK1/2) and p38. Meanwhile, the NF- $\kappa$ B p65 inhibitor ammonium pyrrolidinedithiocarbamate and the ERK1/2 inhibitor U0126, but not the p38 inhibitor SB203580, were able to block oxLDL/ $\beta_2$ GPI/anti- $\beta_2$ GPI complex-induced foam cell formation and migration in A7r5 cells. Hence, it was demonstrated that the oxLDL/ $\beta_2$ GPI/anti- $\beta_2$ GPI complex is able to enhance the lipid uptake, migration and active molecule secretion of A7r5 cells via TLR4, and finally deteriorate atherosclerosis plaques. Additionally, it was demonstrated that oxLDL/ $\beta_2$ GPI/anti- $\beta_2$ GPI complex-induced foam cell formation and migration may be partly mediated by the TLR4/NF- $\kappa$ B signaling pathway and that ERK1/2 may also participate in the process.

*Correspondence to:* Professor Hong Zhou, Jiangsu Key Laboratory of Medicine Science and Laboratory Medicine, School of Medicine, Jiangsu University, 301 Xuefu Road, Zhenjiang, Jiangsu 212013, P.R. China  
E-mail: hongzhou@ujs.edu.cn

\*Contributed equally

**Abbreviations:** AS, atherosclerosis; APS, antiphospholipid syndrome; aPL, antiphospholipid antibodies; anti- $\beta_2$ GPI, anti- $\beta_2$  glycoprotein I;  $\beta_2$ GPI,  $\beta_2$  glycoprotein I; VSMCs, vascular smooth muscle cells; oxLDL, oxidized low-density lipoprotein; TLR4, toll-like receptor 4; NF- $\kappa$ B, nuclear factor  $\kappa$ B; MAPKs, mitogen-activated protein kinases; A7r5, rat thoracic aorta smooth muscle cell line; TF, tissue factor; LPS, lipopolysaccharide; ACAT1, Acetyl-coenzyme A cholesterol acyltransferase; MCP-1, monocyte chemoattractant protein 1; MMP-9, matrix metalloproteinase-9; TC, total cholesterol; FC, free cholesterol; RT, room temperature

**Key words:** oxidized low density lipoprotein/ $\beta_2$  glycoprotein I/anti- $\beta_2$  glycoprotein I complex, vascular smooth muscle cell, foam cell, migration, Toll-like receptor 4

## Introduction

As a complex and chronic inflammatory disease and the main cause of cardiovascular failure, myocardial infarction and stroke, atherosclerosis (AS) is characterized by narrowed arteries, atheromatous plaque formation and destabilization (1). It has been demonstrated that AS is aggravated in autoimmune disorders, including antiphospholipid syndrome (APS) and systemic lupus erythematosus, implying the necessary role of autoimmunity in the mechanism of atherosclerotic progression (2,3).

APS is a systemic autoimmune disease manifested by hypercoagulable states, thromboembolic events and recurrent miscarriage in the presence of antiphospholipid antibodies (aPL), including anti- $\beta_2$ -glycoprotein I antibodies (anti- $\beta_2$ GPI), anticardiolipin antibodies and lupus anticoagulants (4,5). Previous evidence has revealed that the high titer of clinically relevant anti- $\beta_2$ GPI antibodies in the plasma of patients with APS is highly associated with APS-associated vasculopathies and other clinical manifestations (6). As the main antigenic target of aPL,  $\beta_2$ GPI is a protein consisting of

326 amino acid residues and composed of five complementary control domains known as domains I to V. Domains I and IV of  $\beta_2$ GPI have been reported to function as antigen epitopes recognized by antibodies, while domain V has a binding region for negatively charged phospholipids including cardiolipin and oxidative low-density lipoprotein (oxLDL) (7,8). It is widely recognized that oxLDL accumulation in cells of atherosclerotic plaques serves a pivotal pathogenic role in the development of AS (9). OxLDL has proinflammatory and immunological effects that may result in lipid metabolic disturbance and vascular cell dysfunction (10). In 1999,  $\beta_2$ GPI was revealed to co-localize with cluster of differentiation 4-positive lymphocytes and oxidized LDL in human atherosclerotic plaques, suggesting that  $\beta_2$ GPI and anti- $\beta_2$ GPI may participate in the development of thrombosis, particularly in arterial thrombosis (atherosclerosis) (11). In addition, the levels of oxLDL/ $\beta_2$ GPI complex in plasma are notably increased in patients with diseases characterized by cardiovascular complications including systemic autoimmune diseases, diabetes and renal disorders, indicating that oxLDL/ $\beta_2$ GPI is an atherogenic auto-antigen (12,13). Clinical evidence has revealed that the immunoglobulin G (IgG) immune complex containing oxLDL and  $\beta_2$ GPI serves a pathogenic role in the development of thrombosis (14). The coexistence of a stable oxLDL/ $\beta_2$ GPI complex and autoantibodies (anti- $\beta_2$ GPI, anti-oxLDL and anti-oxLDL/ $\beta_2$ GPI) against the complex have been detected in patients with APS (15,16), suggesting the potential of the formation of an oxLDL/ $\beta_2$ GPI/antibodies complex which may be implicated in the atherogenic pathogenesis of AS. In 1997, Hasunuma *et al* (17) demonstrated that a complex composed of oxLDL and  $\beta_2$ GPI is able to be recognized by anti- $\beta_2$ GPI antibodies derived from an *in vivo* model of APS. In addition, Kobayashi *et al* (18), Hasunuma *et al* (17) and Xu *et al* (19) have verified that the co-existence of  $\beta_2$ GPI and anti- $\beta_2$ GPI IgG may substantially enhance the uptake of oxLDL by macrophages. Therefore it was hypothesized that the oxLDL/ $\beta_2$ GPI/anti- $\beta_2$ GPI complex, the combination of the oxLDL/ $\beta_2$ GPI complex and anti- $\beta_2$ GPI, is the circulating immune complex that exerts a pro-atherogenic effect, which has been validated by a number of published studies to a certain extent (3,17-22). Similarly, the effect of the oxLDL/ $\beta_2$ GPI/anti- $\beta_2$ GPI complex on the formation of an atherosclerosis plaque is an interesting topic and may be worth investigating to verify this hypothesis.

Vascular smooth muscle cell (VSMC) is the main cell type involved in the pathogenesis of AS and is closely associated with disease progression due to its interaction with lipoproteins (23). VSMCs exhibit phenotypic and functional plasticity in order to respond to vascular injury (23,24). In the case of vessel damage, VSMCs are able to switch from the quiescent 'contractile' phenotype to the 'synthetic' phenotype (23,24). This change is accompanied by a loss of VSMC markers, an increased capacity for cell proliferation and the migration and secretion of various proinflammatory mediators (24). In contrast to the 'contractile' phenotype which is filled with myofilaments in the cytoplasm, the 'synthetic' phenotype contains a well-developed rough endoplasmic reticulum, which may contribute to the secretion of proinflammatory molecules (24). VSMCs undergoing a phenotype change may additionally acquire macrophage markers and

properties, including the induction of macrophage-specific markers, increased lipid uptake and the ability to present antigens (23,24). It is widely recognized that a heightened inflammatory state serves an essential role in the progression of plaque formation (25,26). Toll-like receptor-4 (TLR4) is a type I trans-membrane pattern recognition receptor which has a critical role in initiating inflammation and particularly participating in immune system activation (27,28). TLR4 has been demonstrated to be involved in the development of AS, particularly at the early stages of the disease (27-30). Nuclear factor kappa B (NF- $\kappa$ B) and mitogen-activated protein kinases (MAPKs) are key signaling molecules for inflammation and immune regulation in arteriosclerosis and are able to mediate the signal transduction pathway of TLRs including TLR4 (31,32). *In vitro* and *in vivo* evidence has implicated the potential function of TLR4 and/or NF- $\kappa$ B and/or MAPKs in a series of physiological changes and inflammatory responses, including foam cell formation, proatherogenic inflammatory cytokines secretion, proliferation and migration (19,21,29-32). However, the detailed association of these transduction signals in VSMCs has not been clearly identified. A full understanding of the behavior of VSMCs in AS with autoimmune backgrounds is critical for the prevention and treatment of arterial thrombosis.

One previous study has demonstrated that the oxLDL/ $\beta_2$ GPI/anti- $\beta_2$ GPI complex may enhance the conversion of macrophages into foam cells and increase the expression of monocyte chemoattractant protein 1 (MCP-1) and tissue factor (TF) via the TLR4/NF- $\kappa$ B pathway (19,21). Considering the different properties between macrophages and VSMCs, the effects of the oxLDL/ $\beta_2$ GPI/anti- $\beta_2$ GPI complex on VSMCs and the underlying molecular mechanisms require further investigation. In the present study, the effects of the oxLDL/ $\beta_2$ GPI/anti- $\beta_2$ GPI complex on the lipid uptake, migration and active molecules secretion of A7r5 cells were investigated, in addition to the potential transduction pathway.

## Materials and methods

**Cell culture.** The A7r5 cell line was obtained from the Shanghai Institutes for Biological Sciences, Chinese Academy of Sciences (Shanghai, China). The cells were maintained in DMEM-F12 medium (Gibco; Thermo Fisher Scientific, Inc., Waltham, MA, USA) supplemented with 10% fetal bovine serum (FBS; Gibco; Thermo Fisher Scientific, Inc.) at 37°C in a humidified incubator with 5% CO<sub>2</sub> and routinely sub-cultured at subconfluency (>90%). Cells were serum starved for 16 h prior to stimulation with oxLDL (50  $\mu$ g/ml; Biomedical Technologies, Inc., Stoughton, MA, USA), oxLDL (50  $\mu$ g/ml)/ $\beta_2$ GPI (100  $\mu$ g/ml; United States Biological, Salem, MA, USA),  $\beta_2$ GPI (100  $\mu$ g/ml)/anti- $\beta_2$ GPI (100  $\mu$ g/ml; Chemicon International, Temecula, CA, USA), oxLDL (50  $\mu$ g/ml)/ $\beta_2$ GPI (100  $\mu$ g/ml)/anti- $\beta_2$ GPI (100  $\mu$ g/ml) or lipopolysaccharide (LPS; 500 ng/ml; Sigma-Aldrich; Merck KGaA, Darmstadt, Germany) at 37°C for 12, 24 or 48 h. The complex of oxLDL/ $\beta_2$ GPI and oxLDL/ $\beta_2$ GPI/anti- $\beta_2$ GPI were prepared by incubating oxLDL (50  $\mu$ g/ml) with  $\beta_2$ GPI (100  $\mu$ g/ml) at 37°C for 16 h as previously described (16). The concentration of the other reagents was determined

by pre-experiments and previous studies (16,19,21). For the interfering corresponding signaling pathway, prior to the aforementioned treatments, the cells were pre-treated at 37°C with 5  $\mu$ M TLR4 inhibitor TAK-242 (Invitrogen; Thermo Fisher Scientific, Inc.), 20  $\mu$ M NF- $\kappa$ B inhibitor ammonium pyrrolidinedithiocarbamate (PDTC; Sigma-Aldrich; Merck KGaA), 10  $\mu$ M p38 inhibitor SB203580 (Sigma-Aldrich; Merck KGaA) and 10  $\mu$ M extracellular regulated kinase 1/2 (ERK1/2) inhibitor U0126 (Selleck Chemicals, Houston, TX, USA) for 2 h. The absence of endotoxin contamination (<0.03 EU/ml) in all reagents (except for LPS) was verified using a Limulus ameocyte lysate kit (Pyrotell; Associates of Cape Cod, Inc., Saint Jean Drive, MA, USA) according to the manufacturers' protocol. Briefly, all reagents (except for LPS) were mixed with pyrochrome at a ratio of 1:1. Then, in a microplate, the pyrochrome-sample mixture was incubated at 37°C for 30 min (100  $\mu$ l/well) and read at 550 nm in an optical reader (Gene Company, Ltd., Hong Kong, China). The endotoxin concentrations were then calculated.

**Oil Red O staining and quantitative analysis of foam cell formation.** The oil red O stock solution was prepared by dissolving 0.5 g oil red O powder (Sigma-Aldrich; Merck KGaA) in 100 ml isopropanol, diluted to 60% with deionized water and filtered as the working solution. A7r5 cells were fixed in 4% paraformaldehyde for 20 min at room temperature (RT). Subsequent to washing with PBS three times, the cells were stained with oil red O working solution at 37°C for 30 min and washed with 60% ethanol for several seconds to remove background staining. Following counterstaining with 10% hematoxylin at RT for 10 min, the stained cells were photographed and evaluated using an inverted optical microscope (Olympus Corporation, Tokyo, Japan) at a magnification of x200. The foam cells were discerned by observing oil red O stained lipid droplets in the cytoplasm.

The foam cell formation was quantitatively analyzed by detecting total intracellular oil red O. In brief, intracellular oil red O was extracted with 100% isopropanol at RT for 30 min, and absorbance of the extraction at 520 nm was measured using a kinetic microplate reader (Gene Company, Ltd., Hong Kong, China). The optical density (OD) was in proportion to the number of positive cells. The cutoff value for a 'high' OD value was calculated by the mean  $\pm$  standard deviation of the media control (DMEM-F12 medium).

**Quantification of intracellular cholesterol content.** Intracellular total cholesterol (TC) and free cholesterol (FC) of A7r5 cells were determined using the Total cholesterol assay kit (cat no. E1015) and Free cholesterol assay kit (cat no. E1016) from Applygen Technologies, Inc. (Beijing, China). In brief, A7r5 cells subsequent to the aforementioned treatments were collected in a centrifuge tube and intracellular lipids were extracted by adding 100  $\mu$ l isopropyl alcohol. Following sonification, the mixtures were centrifuged for 5 min at 2,000  $\times$  g at 4°C. Then, the supernatant was collected for detecting intracellular cholesterol by performing an enzymatic assay according to the manufacturer's protocol of the assay kits. The quantity of TC and FC in the cell extracts were calculated according to the standard curve. Cellular protein concentrations were determined based on a BCA assay by using a BCA Protein

Table I. Primers used in the reverse transcription-quantitative polymerase chain reaction.

Gene	Primer sequence (5'-3')
GADPH (133 bp)	F: GACAACTTTGGCATCGTGGAG R: ATGCAGGGATGATGTTCTGG
ACAT1 (121 bp)	F: AAGTACGCCATCGGCTCTTA R: CTTCTTCACCA CCACGTCT
MMP-9 (356 bp)	F: CCCTGCGTATTTCCATTTCAT R: AAACCCCACTTCTTGTCAGC
MCP-1 (356 bp)	F: TGCTGTCTCAGCCAGATGCAGTTA R: AGAAGTGCTTGAGGTGGTTGTGGAC

F, forward; R, reverse.

Assay kit (cat no. P0011; Beyotime Institute of Biotechnology, Shanghai, China) according to the manufacturer's protocol. The results were then expressed as microgram of cholesterol per milligram of cellular protein. The intracellular cholesterol contents (TC and FC) were normalized with a media control (DMEM-F12 medium).

**Reverse transcription-quantitative polymerase chain reaction (RT-qPCR) analysis.** RT-qPCR was used to assess the mRNA levels of acyl-coenzyme A cholesterol acyltransferase (ACAT1), monocyte chemoattractant protein 1 (MCP-1) and matrix metalloproteinase-9 (MMP-9) following the incubation of A7r5 cells with different treatments as aforementioned. Total RNA was extracted using TRIzol (Invitrogen; Thermo Fisher Scientific, Inc.) and reverse transcribed into cDNA using the Hiscript<sup>TM</sup> First-strand cDNA Synthesis kit (Vazyme, Piscataway, NJ, USA) according to manufacturer's protocol for RT-qPCR analysis. The mRNA level of target genes was examined by RT-qPCR using SYBR Green I dye (Vazyme). The primers used for qPCR were synthesized by Sangon Biotech Co., Ltd. (Shanghai, China) and their sequences were presented in Table I. The PCR assays were performed in triplicate on a Rotor-Gene 2000 Real-Time Quantitative PCR system (Corbett Life Science; Qiagen, Inc., Valencia, CA, USA). The amplification run was performed for 35 cycles under the following conditions: 95°C for 30 sec, 60°C (MCP-1)/60°C (MMP-9)/60°C (GAPDH) for 30 sec and 72°C for 30 sec. The semi-quantitative mRNA level of target gene to GAPDH was calculated using  $2^{-\Delta\Delta C_q}$  method and normalized with a media control (DMEM-F12 medium) (33).

**Wound healing assay.** A wound healing assay was performed as follows: Cells were briefly seeded in 6-well plates and cultured to 95% confluence. The wound gap (100  $\mu$ m) of the cell monolayer was created using a sterile 200- $\mu$ l pipette tip across the diameter, following different treatments as aforementioned. Cell images were obtained immediately and again 48 h later. The images of the wound area were obtained by a light microscope (magnification, x100; Olympus Corporation). The same visual field was marked and used throughout the experiment. The total distance migrated by wounded A7r5

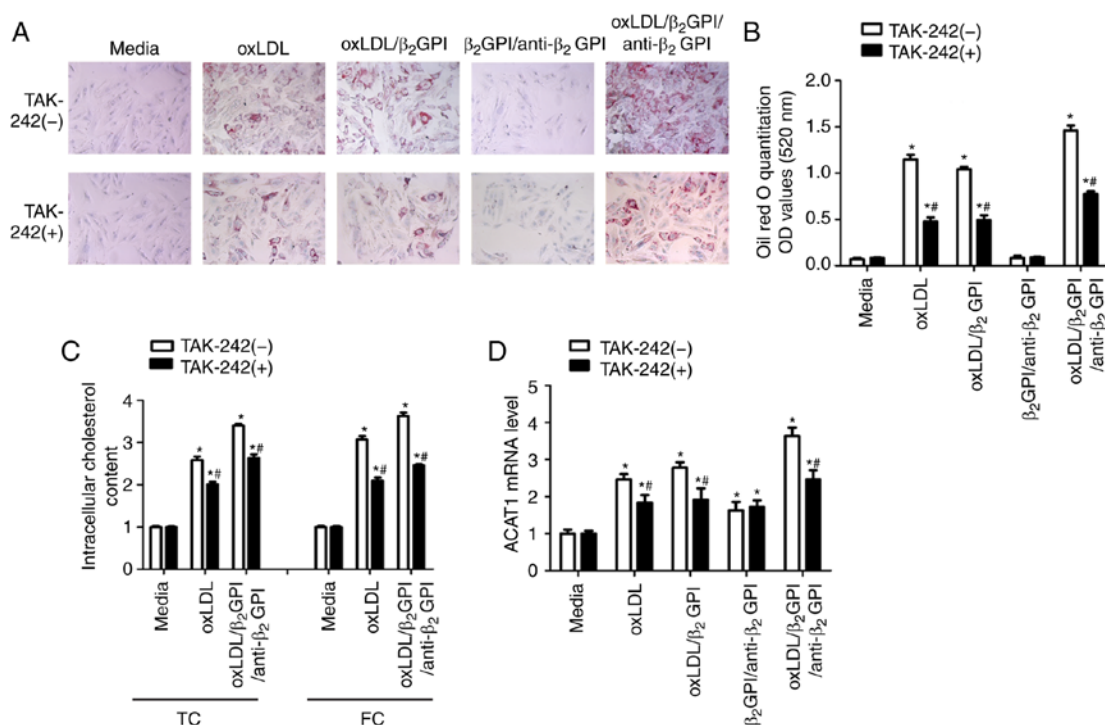


Figure 1. OxLDL/ $\beta_2$ GPI/anti- $\beta_2$ GPI complex induced the lipid accumulation of A7r5 cells via toll-like receptor 4. A7r5 cell was pre-treated with or without TAK-242 for 2 h, then stimulated with oxLDL, oxLDL/ $\beta_2$ GPI,  $\beta_2$ GPI/anti- $\beta_2$ GPI or oxLDL/ $\beta_2$ GPI/anti- $\beta_2$ GPI complex for 48 h. (A) The lipid droplets were stained with Oil Red O and visualized using light microscopy (magnification, x200). (B) The extent of Oil Red O staining was quantified by reading the OD values at 520 nm. (C) TC and FC in A7r5 cells treated with different stimulants were measured. (D) The expression of ACAT1 was detected by reverse transcription-quantitative polymerase chain reaction. The data are expressed as the mean  $\pm$  standard error of the mean (n=5 per group). \*P<0.05 vs. the corresponding media group, #P<0.05 vs. the corresponding group without TAK-242 treatment. OxLDL, oxidized low-density lipoprotein;  $\beta_2$ GPI,  $\beta_2$  glycoprotein I; TLR4, toll-like receptor 4; OD, optical density; ACAT1, Acetyl-coenzyme A cholesterol acyltransferase; TC, total intracellular cholesterol; FC, free cholesterol.

cells was evaluated using ImageJ software (version:1.8.0; National Institutes of Health, Bethesda, MD, USA).

**Transwell migration assay.** A Transwell migration assay was performed using 8- $\mu$ m pore size inserts (Corning Incorporated, Corning, NY, USA) set on 24-well plates. In brief, cell suspensions ( $4 \times 10^4$  cells/well) were added to the upper chamber of the inserts in the presence of different agonists (TAK-242; PDTCT; SB203580 and U0126) and serum-free DMEM-F12 medium, while the lower was filled with DF12 medium containing 10% FBS. After 12 h incubation at 37°C, the non-migrated cells above the membrane were removed using a cotton swab. The membrane was fixed with 4% paraformaldehyde for 20 min at RT, stained with 0.5% crystal violet for 30 min at RT to identify the migrated cells, and photographed with an inverted light microscope (Olympus Corporation) at a magnification of x100. Then, the crystal violet on the membrane was dissolved in 33% acetic acid, and the OD values of the solutions at 570 nm were used to directly assess the cell migration.

**Western blot analysis.** To obtain total cellular proteins, cells incubated with different treatments as aforementioned were lysed in RIPA buffer (P0013K; Beyotime Institute of Biotechnology) containing 1 mM phenylmethylsulfonyl fluoride for 1 h at 4°C. The cell lysates were centrifuged at 13,800  $\times$  g for 10 min at 4°C and stored at -80°C for analysis. Cellular protein concentrations were determined using a BCA Protein Assay kit (cat no. P0011; Beyotime Institute of

Biotechnology) according to the manufacturer's protocol. An equal amount of protein (100  $\mu$ g) was separated by electrophoresis using 10% sodium dodecyl sulfate-polyacrylamide gels and transferred onto polyvinylidene difluoride membranes (PVDF; Bio-Rad Laboratories, Inc., Hercules, CA, USA). Following blocking with fresh 5% fat-free milk for 1 h at RT, PVDF membranes were incubated with the primary antibodies against polyclonal  $\beta$ -actin antibody (1:5,000; cat no. #AP0060; Bioworld Technology, Inc., St. Louis Park, MN, USA), monoclonal rabbit anti-rat TLR4 (1:500; cat no. #sc-76B357.1; Santa Cruz Biotechnology, Inc., Dallas, TX, USA), monoclonal rabbit anti-rat NF- $\kappa$ B p65 (1:1,000; cat no. #8242; Cell Signaling Technology, Inc., Danvers, MA, USA), monoclonal rabbit anti-rat phosphorylated (phospho)-NF- $\kappa$ B-p65 ser536 (1:1,000; cat no. #3033; Cell Signaling Technology, Inc.), monoclonal mouse anti-rat ERK1/2 (1:1,000; cat no. #sc-514302; Santa Cruz Biotechnology, Inc.), monoclonal mouse anti-rat phospho-ERK1/2 (1:1,000; cat no. #sc-7388; Santa Cruz Biotechnology, Inc.), monoclonal mouse anti-rat p38 (1:1,000; cat no. #sc-7972; Santa Cruz Biotechnology, Inc.), monoclonal mouse anti-rat phospho-p38 (1:1,000; cat no. #sc-166182; Santa Cruz Biotechnology, Inc.) overnight at 4°C. Following washing with PBS for 10 min three times, the membranes were then incubated with horseradish peroxidase-conjugated goat anti-rabbit (1:5,000; cat no. BS13278; Bioworld Technology, Inc.) or anti-mouse (1:5,000; cat no. #API24P; EMD Millipore, Billerica, MA, USA) secondary antibodies for 1 h at RT. Finally, the protein bands were visualized using electrochemiluminescence detection reagents (GE Healthcare, Chicago,

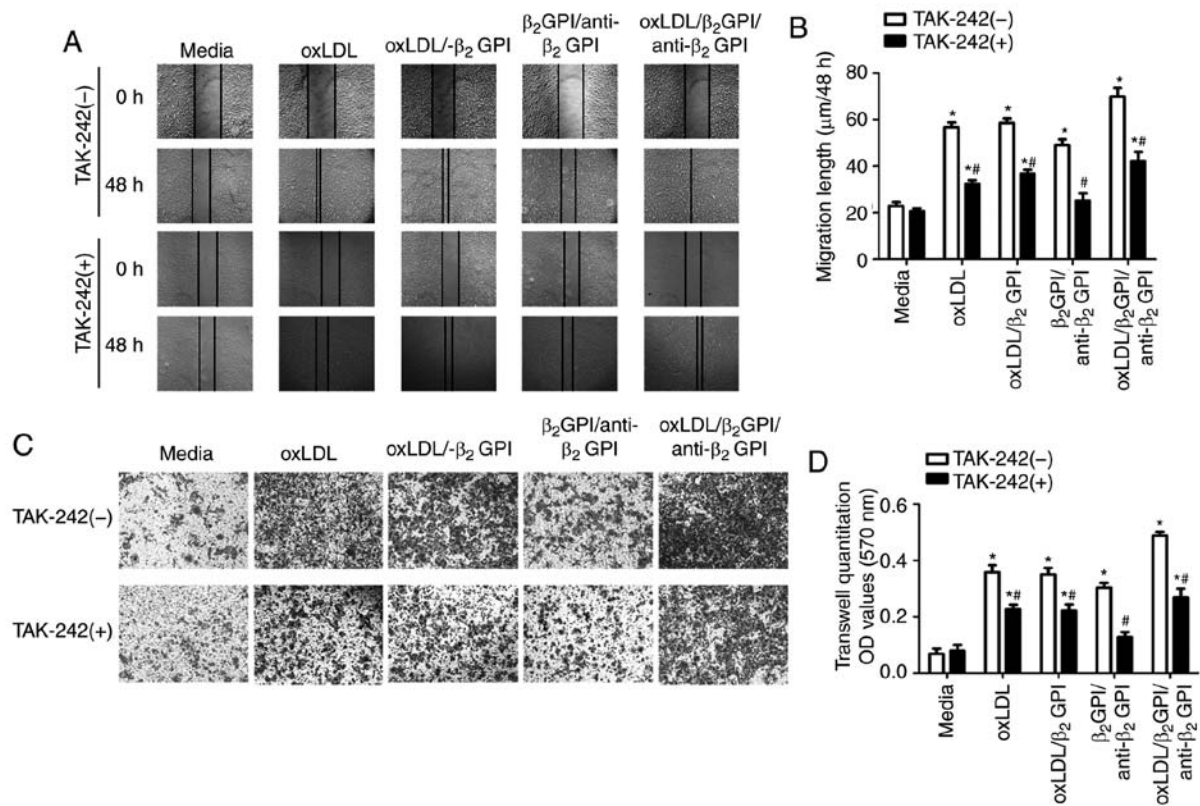


Figure 2. OxLDL/ $\beta_2$ GPI/anti- $\beta_2$ GPI complex induced the migration of A7r5 cells via toll-like receptor 4. A7r5 cell was pre-treated with or without TAK-242 for 2 h, then stimulated with oxLDL, oxLDL/ $\beta_2$ GPI,  $\beta_2$ GPI/anti- $\beta_2$ GPI or oxLDL/ $\beta_2$ GPI/anti- $\beta_2$ GPI complex for 48 or 12 h respectively. (A) A wound healing assay of A7r5 cells treated with different stimulants for 48 h was performed and (B) quantified. A7r5 cells were then seeded into the upper chamber of a Transwell insert. Trans-membrane cells were (C) stained with crystal violet and (D) quantified by reading the absorbance at 570 nm after 12 h. The data are expressed as the mean  $\pm$  standard error of the mean (n=5 per group). \*P<0.05 vs. the corresponding media group, #P<0.05 vs. the corresponding group without TAK-242 treatment. OxLDL, oxidized low-density lipoprotein;  $\beta_2$ GPI,  $\beta_2$  glycoprotein I; OD, optical density.

IL, USA) and imaged using an ImageQuant LAS 4000 Imager and quantitated by Labwork version 4.6 (UVP, LLC, Phoenix, AZ, USA).

**Enzyme-linked immunosorbent assay (ELISA).** A7r5 cells were seeded at a density of  $1.0 \times 10^5$ /well in a 96-well plate. Subsequent to being serum-starved for 16 h, cells were treated with different stimulants as aforementioned. Cells in certain wells were pretreated with TAK-242 (5  $\mu$ M) for 2 h, MCP-1 and MMP-9 secreted into the cell culture media was measured using MCP-1 ELISA kit (cat no. ERC 113; Neobioscience Technology, Co., Ltd., Shenzhen, Guangdong, China) and MMP-9 ELISA kit (cat no. ERC 018; Neobioscience Technology, Co., Ltd.) according to the manufacturer's protocol. The protein levels were expressed as pg/ml in cell culture media.

**Statistical analysis.** All experiments were performed in triplicate or quadruplicate and repeated at least 3 times. Data were expressed as the mean  $\pm$  standard error of the mean. Statistical significance was examined using a Student's unpaired t-test (two tailed) for two-group comparisons and one-way analysis of variance with Dunnett's post-test. for multiple-group comparisons. Statistical evaluation was performed using SPSS statistical software package version 20.0 (IBM Corp., Armonk, NY, USA). P<0.05 was considered to indicate a statistically significant difference.

## Results

*OxLDL/ $\beta_2$ GPI/anti- $\beta_2$ GPI complex promotes the lipid uptake of A7r5 cells and the involvement of TLR4.* To investigate whether the oxLDL/ $\beta_2$ GPI/anti- $\beta_2$ GPI complex may enhance the lipid accumulation of A7r5 cells and include the involvement of TLR4, the cells were incubated with different stimuli (media, oxLDL, oxLDL/ $\beta_2$ GPI,  $\beta_2$ GPI/anti- $\beta_2$ GPI or oxLDL/ $\beta_2$ GPI/anti- $\beta_2$ GPI complex) for 48 h. Oil Red O staining and intracellular cholesteryl quantitation were performed to assess the capability of lipid uptake. As presented in Fig. 1, oxLDL was essential for the foam cell formation, as confirmed by intensive lipid droplets in the cytoplasm stained with Oil Red O and high OD values (P<0.05 vs. media group; Fig. 1B). More notably, compared with the control groups, A7r5 cells in the oxLDL/ $\beta_2$ GPI/anti- $\beta_2$ GPI complex group presented a significantly greater number of lipid droplets (P<0.05 vs. oxLDL and oxLDL/ $\beta_2$ GPI group; Fig. 1B) and increased intracellular cholesterol level (TC and FC; P<0.05 vs. oxLDL group; Fig. 1C). Furthermore, when cells were pretreated with TAK-242, which is able to specifically bind to TLR4 to interfere with the interactions between TLR4 and its adaptor molecules, the lipid accumulation of A7r5 cells in all groups containing oxLDL were partially but significantly attenuated (P<0.05 vs. the corresponding group without TAK-242 treatment; Fig. 1A-C). Similarly, the mRNA levels of ACAT1, which is a key and exclusive enzyme involved

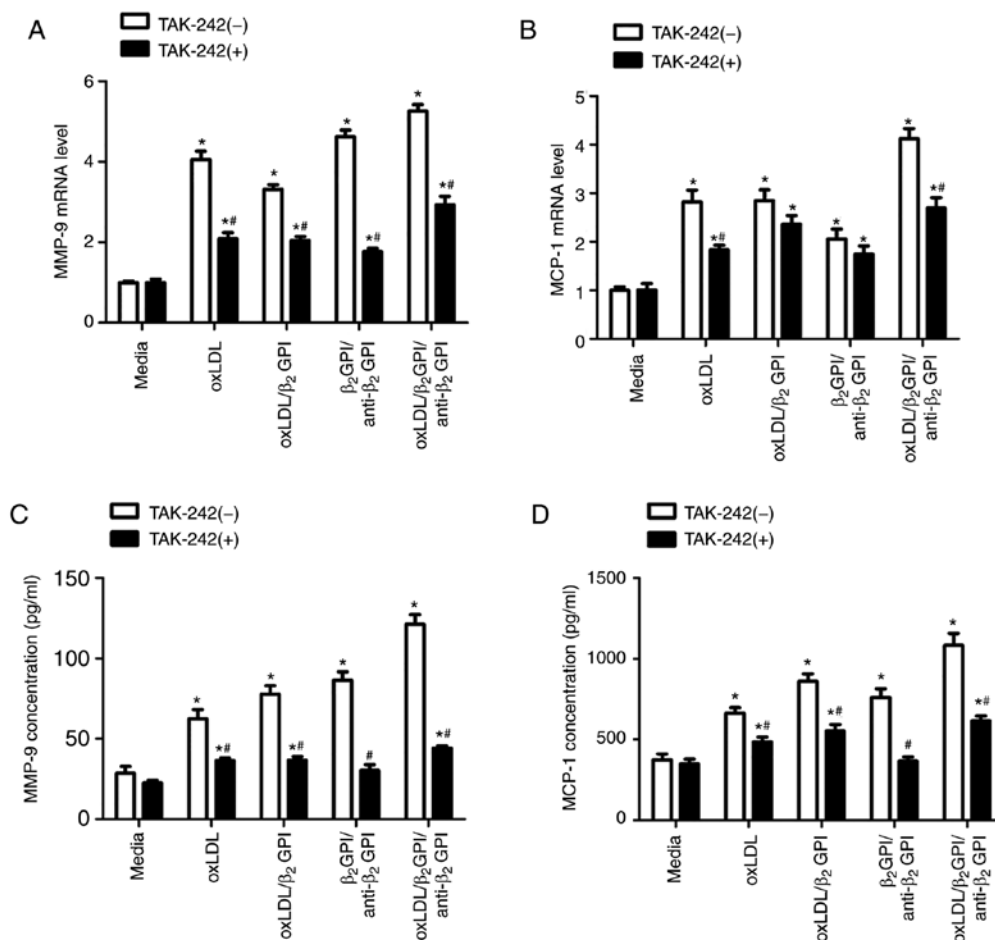


Figure 3. Involvement of toll-like receptor 4 in the oxLDL/ $\beta_2$ GPI/anti- $\beta_2$ GPI complex-induced expression of MMP-9 and MCP-1. A7r5 cells were pre-treated with or without TAK-242 for 2 h, then stimulated with oxLDL, oxLDL/ $\beta_2$ GPI,  $\beta_2$ GPI/anti- $\beta_2$ GPI or oxLDL/ $\beta_2$ GPI/anti- $\beta_2$ GPI complex for (A and B) 12 or (C and D) 48 h. Total RNA of cells was extracted for detecting (A) MMP-9 and (B) MCP-1 mRNA by reverse transcription-quantitative polymerase chain reaction. The cell cultural supernatants were collected for analyzing the secretion of (C) MMP-9 and (D) MCP-1 using commercial enzyme-linked immunosorbent assay kits. The data are expressed as the mean  $\pm$  standard error of the mean (n=5 per group). \*P<0.05 vs. the corresponding media group, #P<0.05 vs. the corresponding group without TAK-242 treatment. OxLDL, oxidized low-density lipoprotein;  $\beta_2$ GPI,  $\beta_2$  glycoprotein I; MMP-9, matrix metalloproteinase-9; MCP-1, monocyte chemoattractant protein 1.

in intracellular cholesteryl esterification, was increased more substantially in the oxLDL/ $\beta_2$ GPI/anti- $\beta_2$ GPI complex group compared with the control group (P<0.05 vs. oxLDL, oxLDL/ $\beta_2$ GPI and  $\beta_2$ GPI/anti- $\beta_2$ GPI group, Fig. 1D), while the upregulated ACAT1 expression was partly blocked in the TAK-242-treated oxLDL/ $\beta_2$ GPI/anti- $\beta_2$ GPI complex group (P<0.05 vs. media and oxLDL/ $\beta_2$ GPI/anti- $\beta_2$ GPI complex group without TAK-242 treatment; Fig. 1D). Additionally, the apparent inhibitory effects of TAK-242 on ACAT1 mRNA expression were also present in the oxLDL and oxLDL/ $\beta_2$ GPI groups (P<0.05 vs. media and the corresponding group without TAK-242 treatment; Fig. 1D).

**OxLDL/ $\beta_2$ GPI/anti- $\beta_2$ GPI complex induced A7r5 cell migration and the involvement of TLR4.** To reveal whether the oxLDL/ $\beta_2$ GPI/anti- $\beta_2$ GPI complex is able to promote A7r5 cell migration via TLR4, a wound healing assay (Fig. 2A and B) and a Transwell migration assay (Fig. 2C and D) were performed to assess the cell migratory ability. The results revealed that the oxLDL/ $\beta_2$ GPI/anti- $\beta_2$ GPI complex was able to substantially enhance A7r5 cell migration when compared with the control groups (P<0.05 vs. oxLDL, oxLDL/ $\beta_2$ GPI

and  $\beta_2$ GPI/anti- $\beta_2$ GPI group; Fig. 2B and D). Furthermore, pre-treatment with a TLR4 inhibitor (TAK-242) partly attenuated the promotion of migration in oxLDL, oxLDL/ $\beta_2$ GPI and oxLDL/ $\beta_2$ GPI/anti- $\beta_2$ GPI complex groups (P<0.05 vs. media and the corresponding group without TAK-242 treatment), whereas the effect of  $\beta_2$ GPI/anti- $\beta_2$ GPI on migration was completely blocked (P<0.05 vs.  $\beta_2$ GPI/anti- $\beta_2$ GPI group without TAK-242 treatment and P>0.05 vs. media group; Fig. 2B and D).

**Involvement of TLR4 in the oxLDL/ $\beta_2$ GPI/anti- $\beta_2$ GPI complex upregulated pro-atherogenic molecule expression.** MMP-9 is one of the major MMPs secreted by VSMCs, which is activated and upregulated in atherosclerotic lesions, contributing to the migration of VSMCs by degrading the extracellular matrix (34). MCP-1, which is synthesized by several activated vascular cells, is able to recruit circulating monocytes to the plaque area and result in a greater number of foam cells forming and the aggravation of vascular inflammation (35). In the present study, the effects of the oxLDL/ $\beta_2$ GPI/anti- $\beta_2$ GPI complex on the expression of MCP-1 and MMP-9 were investigated. The results revealed

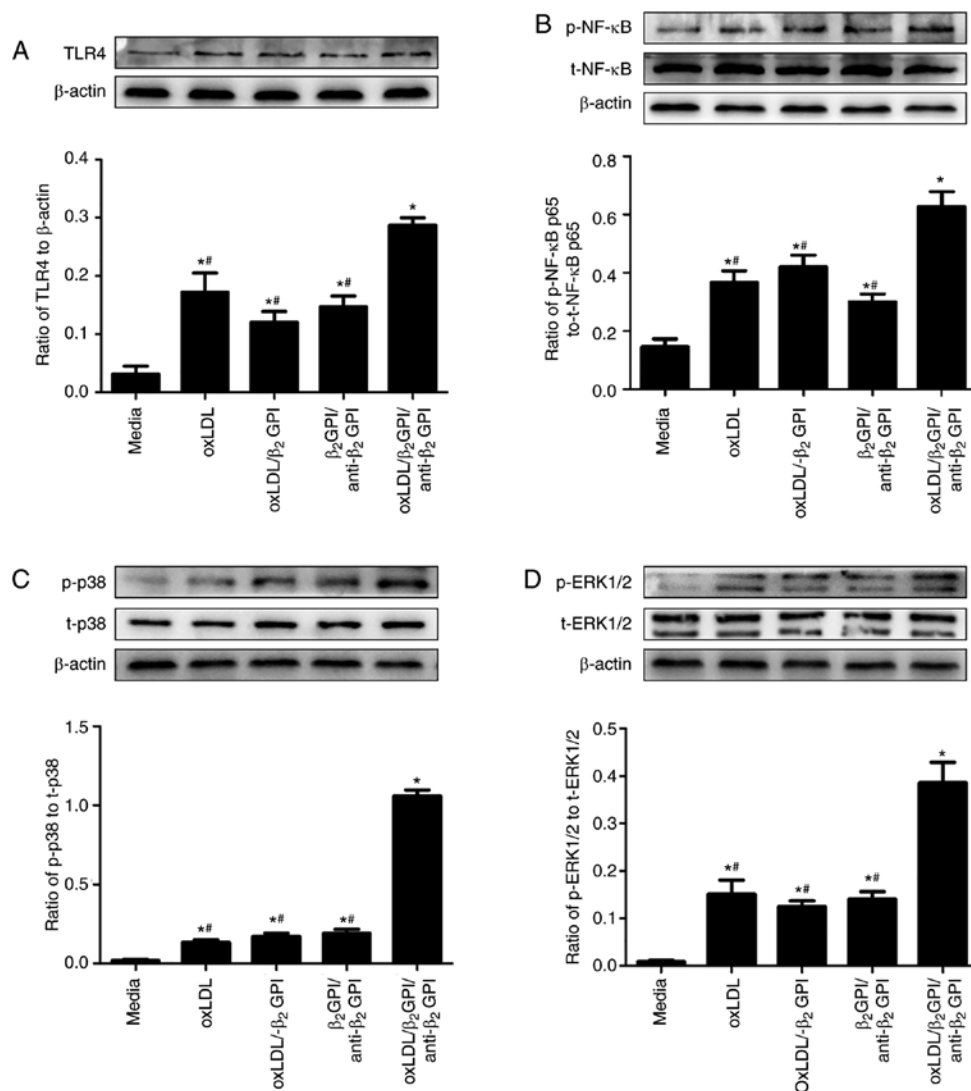


Figure 4. Activation of TLR4 and downstream signaling molecules during the stimulation of oxLDL/ $\beta_2$ GPI/anti- $\beta_2$ GPI in A7r5 cells. A7r5 cells were treated with oxLDL, oxLDL/ $\beta_2$ GPI,  $\beta_2$ GPI/anti- $\beta_2$ GPI and oxLDL/ $\beta_2$ GPI/anti- $\beta_2$ GPI complex for (A and B) 24 or (C and D) 48 h. Cell lysates were collected for analyzing (A) TLR4 expression and the phosphorylation of (B) NF- $\kappa$ B p65, (C) p38 and (D) ERK1/2 by western blot analysis. The data are expressed as the mean  $\pm$  standard error of the mean (n=5 per group). \*P<0.05 vs. the corresponding media group, #P<0.05 vs. the oxLDL/ $\beta_2$ GPI/anti- $\beta_2$ GPI complex group. TLR4, toll-like receptor 4; OxLDL, oxidized low-density lipoprotein;  $\beta_2$ GPI,  $\beta_2$  glycoprotein I; p-, phosphorylated; t-, total; NF- $\kappa$ B, nuclear factor- $\kappa$ B; ERK1/2, extracellular-regulated kinase 1/2.

that oxLDL, oxLDL/ $\beta_2$ GPI and  $\beta_2$ GPI/anti- $\beta_2$ GPI in addition to the oxLDL/ $\beta_2$ GPI/anti- $\beta_2$ GPI complex were able to increase MCP-1 and MMP-9 mRNA expression and protein secretion compared with the media control (P<0.05 vs. media; Fig. 3), and the effects of the oxLDL/ $\beta_2$ GPI/anti- $\beta_2$ GPI complex were more notable compared with any other group (P<0.05 vs. oxLDL, oxLDL/ $\beta_2$ GPI and  $\beta_2$ GPI/anti- $\beta_2$ GPI group; Fig. 3). To investigate whether TLR4 was involved in mediating this process, A7r5 cells were pre-treated with TLR4 inhibitor TAK-242 prior to other treatments. The data revealed that TAK-242 was able to partly decrease the mRNA and protein expression of MCP-1 and MMP-9 in the oxLDL and oxLDL/ $\beta_2$ GPI/anti- $\beta_2$ GPI complex groups, in addition to the oxLDL/ $\beta_2$ GPI-induced protein expression (P<0.05 vs. media and the corresponding group without TAK-242 treatment; Fig. 3). However, the effect of  $\beta_2$ GPI/anti- $\beta_2$ GPI on the protein secretion of MMP-9 and MCP-1 was completely blocked by TAK-242 (P<0.05 vs.  $\beta_2$ GPI/anti- $\beta_2$ GPI group

without TAK-242 treatment and P>0.05 vs. media group; Fig. 3C and D).

**Function of TLR4 in oxLDL/ $\beta_2$ GPI/anti- $\beta_2$ GPI complex-stimulated phosphorylation of NF- $\kappa$ B and MAPKs.** TLR4-mediated signal transduction has been reported to participate in VSMCs pathogenesis of AS (27,29,30,32). The results of the present study also confirmed that the oxLDL/ $\beta_2$ GPI/anti- $\beta_2$ GPI complex is able to induce A7r5 cell foam cell formation, migration and active molecule secretion, which were partly mediated by TLR4. Subsequently, the effects of the oxLDL/ $\beta_2$ GPI/anti- $\beta_2$ GPI complex on TLR4 expression and the phosphorylation of NF- $\kappa$ B and MAPKs in A7r5 cells were investigated to further clarify the participation of TLR4-mediated signal transduction in a series of pro-atherogenic phenotypes. As presented in Fig. 4A, cells treated with the oxLDL/ $\beta_2$ GPI/anti- $\beta_2$ GPI complex had a significantly increased expression of TLR4 protein (P<0.05 vs. media,



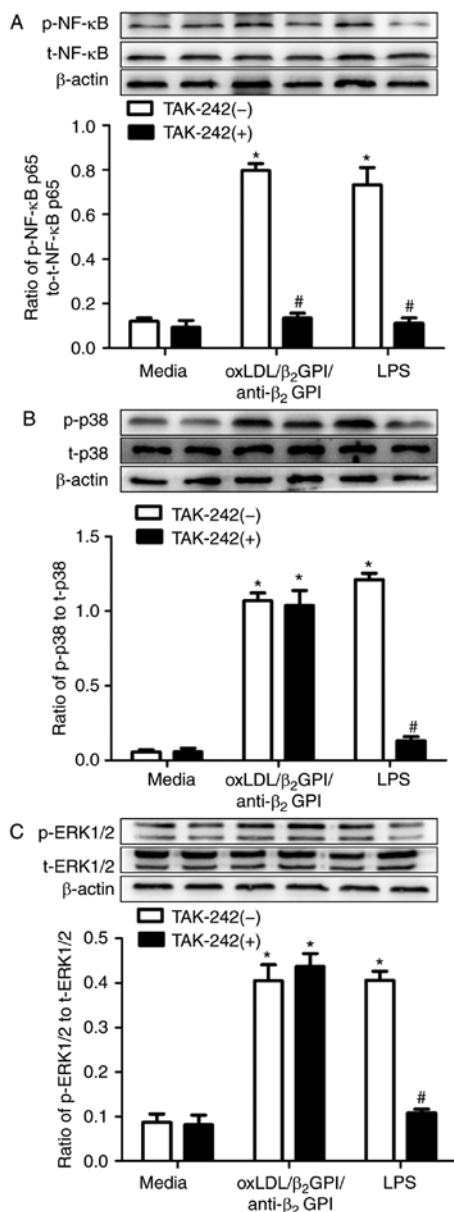


Figure 5. Involvement of toll-like receptor 4 in oxLDL/ $\beta_2$ GPI/anti- $\beta_2$ GPI complex-stimulated phosphorylation of NF- $\kappa$ B and mitogen-activated protein kinases during the formation of foam cells. A7r5 cells were treated with oxLDL/ $\beta_2$ GPI/anti- $\beta_2$ GPI complex and LPS with or without TAK-242 pre-treatment. Western blot analysis was performed to assess the phosphorylation of (A) NF- $\kappa$ B p65, (B) p38 and (C) ERK1/2. The data are expressed as the mean  $\pm$  standard error of the mean (n=5 per group). \*P<0.05 vs. the corresponding media group, #P<0.05 vs. the corresponding group without TAK-242 treatment. OxLDL, oxidized low-density lipoprotein;  $\beta_2$ GPI,  $\beta_2$  glycoprotein I; p-, phosphorylated; t-, total; NF- $\kappa$ B, nuclear factor- $\kappa$ B; ERK1/2, extracellular-regulated kinase 1/2; LPS, lipopolysaccharide.

oxLDL, oxLDL/ $\beta_2$ GPI and  $\beta_2$ GPI/anti- $\beta_2$ GPI group). Similarly, the positive effects of the oxLDL/ $\beta_2$ GPI/anti- $\beta_2$ GPI complex on the phosphorylation of NF- $\kappa$ B p65, ERK1/2 and p38 were more notable compared with any other stimulants (P<0.05 vs. media, oxLDL, oxLDL/ $\beta_2$ GPI and  $\beta_2$ GPI/anti- $\beta_2$ GPI group; Fig. 4B-D).

To further delineate the role of TLR4 in the oxLDL/ $\beta_2$ GPI/anti- $\beta_2$ GPI complex-induced phosphorylation of signaling transduction molecules, cells were pre-treated with TAK-242 prior to other treatments. As presented in Fig. 5, TAK-242 was able to decrease the phosphorylation

levels of NF- $\kappa$ B p65 in oxLDL/ $\beta_2$ GPI/anti- $\beta_2$ GPI complex and LPS-treated groups compared with the control group (P<0.05 vs. the corresponding group without TAK-242; Fig. 5A). LPS, the natural ligand of TLR4, is widely confirmed to trigger the downstream transduction pathway of TLR4 (36). Of note, the phosphorylation of ERK1/2 and p38 may not be attenuated by TAK-242 in oxLDL/ $\beta_2$ GPI/anti- $\beta_2$ GPI complex treated group (P>0.05 vs. oxLDL/ $\beta_2$ GPI/anti- $\beta_2$ GPI complex group without TAK-242; Fig. 5A) while the effects of LPS were completely blocked (P<0.05 vs. LPS group without TAK-242; Fig. 5C).

*PDTC and U0126 attenuated the effects of the oxLDL/ $\beta_2$ GPI/anti- $\beta_2$ GPI complex on foam cell formation and migration in A7r5 cells.* The above results revealed that TLR4, NF- $\kappa$ B, p38 and ERK1/2 may be involved in oxLDL/ $\beta_2$ GPI/anti- $\beta_2$ GPI complex-induced lipid accumulation and migration in A7r5 cells. To further address these results, cells were pre-incubated with PDTC, SB203580 and U0126 to suppress the activation of NF- $\kappa$ B, p38 and ERK1/2, respectively, and the changes in lipid uptake and migration of cells stimulated by the oxLDL/ $\beta_2$ GPI/anti- $\beta_2$ GPI complex were observed. As presented in Fig. 6, PDTC and U0126 pretreatment partly attenuated the pro-atherosclerotic activities (foam cell formation and migration) of A7r5 cells (P<0.05 vs. oxLDL/ $\beta_2$ GPI/anti- $\beta_2$ GPI complex group without inhibitors; Fig. 6B and D). However, the effects of the oxLDL/ $\beta_2$ GPI/anti- $\beta_2$ GPI complex on cells were not normalized by SB203580 (P>0.05 vs. oxLDL/ $\beta_2$ GPI/anti- $\beta_2$ GPI complex group without inhibitors; Fig. 6B and D).

## Discussion

AS may result in the dysfunction of vascular cells, arteries lesions and atheroma formation and is the pathological foundation of numerous cardiovascular diseases (37,38). The roles of inflammatory reactions and immune system activation in AS have been investigated in previous research (30,31,39). Growing evidence has demonstrated that AS has an autoimmune nature and autoimmunity serves an important role in atherogenesis (3,40). Accumulating evidence supports the hypothesis that the oxLDL/ $\beta_2$ GPI/anti- $\beta_2$ GPI complex, a potential pro-atherogenic immune complex, is the circulating immune complex that exerts a pro-atherogenic effect in patients with AS with APS (3,17-22). The pro-atherogenic activation of macrophages induced by the oxLDL/ $\beta_2$ GPI/anti- $\beta_2$ GPI complex, in addition to the underlying mechanism, have been investigated previously (17-20). However, the effect of the oxLDL/ $\beta_2$ GPI/anti- $\beta_2$ GPI complex on other vascular cells, particularly VSMCs, and the precise mechanism involved has not been unequivocally elucidated.

In the progression of AS, VSMCs exhibit phenotypic switching, including migration and foam cell formation, in response to vascular injury (24). In advanced AS plaque, the majority of foam cells displayed VSMC markers, with only 30% presenting a macrophage phenotype whereas 45% presented a VSMC phenotype, indicating that the foam cell formation of VSMCs is a fundamental process in the pathology of AS (41). Subsequent to migrating into the intima, VSMCs accumulate excessive oxLDL in the cytoplasm and transform into foam cells, which contribute to AS progression (23,24). In the



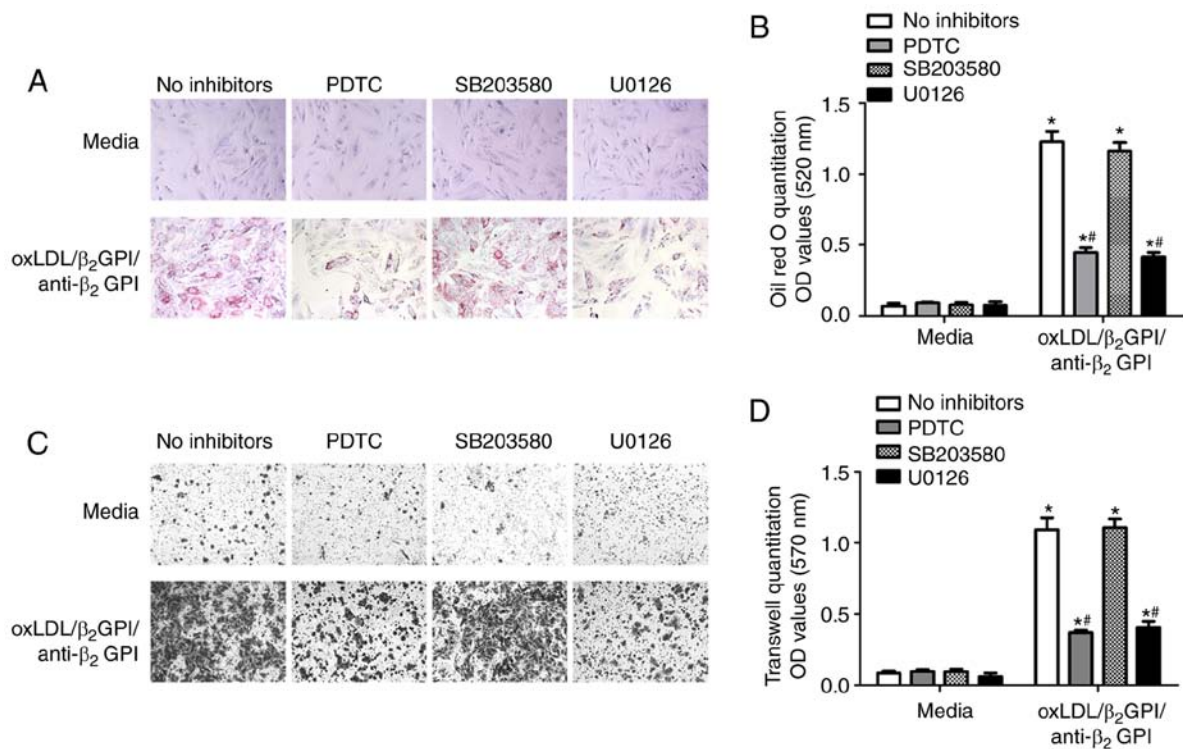


Figure 6. PDTC and U0126 attenuated the oxLDL/β<sub>2</sub>GPI/anti-β<sub>2</sub>GPI complex-induced foam cell formation and migration of A7r5 cell. Cells were pre-treated with or without PDTC, SB203580 and U0126 for 2 h, then stimulated with oxLDL/β<sub>2</sub>GPI/anti-β<sub>2</sub>GPI complex for 48 and 12 h. (A) Foam cells formation (B) quantified, and (C) the migration (D) quantified of A7r5 cells were presented. The data are expressed as the mean ± standard error of the mean (n=5 per group). \*P<0.05 vs. corresponding media group, \*\*P<0.05 vs. corresponding group without inhibitors treatment. OxLDL, oxidized low-density lipoprotein; β<sub>2</sub>GPI, β<sub>2</sub> glycoprotein I; PDTC, ammonium pyrrolidinedithiocarbamate; OD, optical density.

advanced stage of AS, the apoptosis and necrosis of foam cells result in the structural complexity and rupture of the atherosclerotic plaque, ultimately resulting in serious cardiovascular events (23,24). ACAT1, whose activity is present in a variety of cells and tissues, is an intracellular enzyme that converts FC into cholesteryl esters for storage in lipid droplets, promoting foam cell formation in atherosclerotic lesions (42,43). It is well-accepted that the expression of ACAT1 promotes intracellular lipid accumulation and ultimately results in foam cell formation in macrophages and smooth muscle cells (29,44). In the present study, whether the oxLDL/β<sub>2</sub>GPI/anti-β<sub>2</sub>GPI complex was able further enhance the lipid uptake capabilities of A7r5 cells compared with oxLDL alone and other control stimuli was examined; additionally, the function of TLR4 in the phagocytosis of the oxLDL/β<sub>2</sub>GPI/anti-β<sub>2</sub>GPI complex in A7r5 cells was verified. Firstly, Oil Red staining and intracellular cholesterol measurement results suggested a more aggressive effect of the oxLDL/β<sub>2</sub>GPI/anti-β<sub>2</sub>GPI complex on lipid uptake in A7r5 cells (Fig. 1A-C). The data also reveal that the oxLDL/β<sub>2</sub>GPI/anti-β<sub>2</sub>GPI complex may significantly upregulate the expression of ACAT1 mRNA, implying the involvement of ACAT1 in complex-induced VSMCs foam cell formation (P<0.05 vs. oxLDL, oxLDL/β<sub>2</sub>GPI and β<sub>2</sub>GPI/anti-β<sub>2</sub>GPI group; Fig. 1D). Recently, a number of receptors involved in oxLDL uptake have been reported, including scavenger receptors, lectin-like oxidized low-density lipoprotein receptor-1 and TLRs (4,45). The expression of these receptors on the surface of vascular wall cells (endothelial cells, macrophages and VSMCs) initiates the cellular effects of oxLDL.

It is reported that TLR4 is able to facilitate oxLDL-induced inflammatory secretion and migration, in addition to the foam cell formation of VSMCs (29,46). In support of this, the results of the present study revealed that the oxLDL/β<sub>2</sub>GPI/anti-β<sub>2</sub>GPI complex-induced lipid accumulation and ACAT1 mRNA expression of A7r5 cells were partly blocked by a TLR4 inhibitor, providing evidence for the hypothesis that the oxLDL/β<sub>2</sub>GPI/anti-β<sub>2</sub>GPI complex-enhanced lipid uptake in A7r5 cells is partially mediated by TLR4, and that ACAT1 participates in the process (Fig. 1). Noteworthy, similar effects were also presented in other groups containing oxLDL, which were consistent with a previous study in which the authors demonstrated that oxLDL was able to promote foam cell formation of vascular smooth muscle cells by upregulating TLR4-mediated ACAT1 expression (29). It may be explained by the fact that oxLDL and the oxLDL/β<sub>2</sub>GPI/anti-β<sub>2</sub>GPI complex, to some degree, share a common signaling pathway in inducing the foam cell formation of VSMCs.

The aberrant migration of VSMCs is regarded as a key mechanism for the development of the initial thickening and the progression of the thickened intima to an fibroatheroma or fibrous plaque (23). MMP-9 and MCP-1 are able to promote VSMC migration from the tunica media into the intima and the infiltration of macrophages, respectively, which are the earliest events in formation of arterial plaques (47,48). In the present study, the effect of the oxLDL/β<sub>2</sub>GPI/anti-β<sub>2</sub>GPI complex on migration, MMP-9 and MCP-1 secretion during the process of VSMC foam cell formation was examined. The results demonstrated that the oxLDL/β<sub>2</sub>GPI/anti-β<sub>2</sub>GPI

complex was able to further potentiate the A7r5 cell migration ability and the expression of MMP-9 (Figs. 2 and 3). In addition, the oxLDL/ $\beta_2$ GPI/anti- $\beta_2$ GPI complex had the strongest effect on MCP-1 expression in A7r5 cells when compared with other control groups (Fig. 3). The present study further confirmed the involvement of TLR4 in the oxLDL/ $\beta_2$ GPI/anti- $\beta_2$ GPI complex-induced migration and MMP-9 and MCP-1 expression of cells through the use of TAK-242. Treatment with TAK-242 partly inhibited oxLDL, oxLDL/ $\beta_2$ GPI and oxLDL/ $\beta_2$ GPI/anti- $\beta_2$ GPI complex-induced migration, but completely inhibited the effect of  $\beta_2$ GPI/anti- $\beta_2$ GPI (Figs. 2 and 3). Similarly, TLR4 inhibition partially impeded the effect of oxLDL, oxLDL/ $\beta_2$ GPI and the oxLDL/ $\beta_2$ GPI/anti- $\beta_2$ GPI complex on MMP-9 and MCP-1 expression whereas the  $\beta_2$ GPI/anti- $\beta_2$ GPI-induced effect was completely diminished. However, the inhibitory effect of TAK-242 on MMP-9 and MCP-1 mRNA expression was not as notable compared with the effect on the protein secreted into the supernatant, which may be explained by post-translational modifications (Fig. 3). Altogether, these results demonstrated that the oxLDL/ $\beta_2$ GPI/anti- $\beta_2$ GPI complex and oxLDL, in addition to oxLDL/ $\beta_2$ GPI, induced migration and pro-atherogenic molecule secretion in the process of A7r5 cell foam cell formation, which were partly mediated by TLR4. In addition, the function of TLR4 in the  $\beta_2$ GPI/anti- $\beta_2$ GPI induced molecule activation was verified, which is consistent with previous results in THP-1 cells and macrophages (19,21,49).

Regarding the signaling molecules that are involved in the TLR4-modulated VSMC pro-atherogenic activation, the present study focused on the function of NF- $\kappa$ B and MAPKs. As aforementioned, NF- $\kappa$ B and MAPKs have been reported to be involved in pro-atherogenic behaviors, including foam cell formation, migration and inflammatory cytokine synthesis (19,21,29,30,32). Although still not fully elucidated, the precise signaling transduction mechanism underlying VSMC foam cell formation and migration has attracted increasing attention (29,50). Particularly, the TLR4 downstream cascade that was implicated in the effects of the oxLDL/ $\beta_2$ GPI/anti- $\beta_2$ GPI complex needs to be further determined.

In order to elucidate this, TLR4 expression and the phosphorylation of NF- $\kappa$ B and MAPKs with or without TAK-242 were detected during treatment with the oxLDL/ $\beta_2$ GPI/anti- $\beta_2$ GPI complex. It was revealed that TLR4 protein expression and the relative phosphorylation level of NF- $\kappa$ B p65, ERK1/2 and p38 were largely increased during stimulation with the oxLDL/ $\beta_2$ GPI/anti- $\beta_2$ GPI complex and the activation of NF- $\kappa$ B p65 was dependent on TLR4 activation (Fig. 4A-D). Of note, the oxLDL/ $\beta_2$ GPI/anti- $\beta_2$ GPI complex had no effect on the phosphorylation of JNK (data not shown) and TAK-242 was unable to decrease the effect of the oxLDL/ $\beta_2$ GPI/anti- $\beta_2$ GPI complex on the activation of ERK1/2 and p38 (Fig. 5). These unanticipated observations suggest that there may be multiple receptors mediating oxLDL/ $\beta_2$ GPI/anti- $\beta_2$ GPI complex-induced pro-atherogenic behaviors, including TLR2 and Fc $\gamma$  receptors. Furthermore, inhibitors of NF- $\kappa$ B, ERK1/2 and p38 were used to verify their involvement in oxLDL/ $\beta_2$ GPI/anti- $\beta_2$ GPI complex-induced VSMC phenotypic switching. It was revealed that the oxLDL/ $\beta_2$ GPI/anti- $\beta_2$ GPI complex-induced foam cell forma-

tion and migration of A7r5 cells were partly impaired by PDTC and U0126, but not SB203580 (Fig. 5). These results clearly demonstrate that oxLDL/ $\beta_2$ GPI/anti- $\beta_2$ GPI complex-induced A7r5 cell foam cell formation and migration are partly mediated by the TLR4/NF- $\kappa$ B signaling pathway and that ERK1/2 is also involved in the process.

The importance of the present study is that it is the first study, to the best of our knowledge, to certify the effect of three complexes, composed of APS-associated pathogenic anti- $\beta_2$ GPI,  $\beta_2$ GPI and atherogenic oxLDL, on the lipid uptake, migration and active molecule expression of VSMCs. Although it may be concluded that oxLDL is the primary component of the oxLDL/ $\beta_2$ GPI/anti- $\beta_2$ GPI complex, the effects of  $\beta_2$ GPI and anti- $\beta_2$ GPI cannot be ignored. The importance of the function of  $\beta_2$ GPI and anti- $\beta_2$ GPI may be demonstrated by the stronger effect of the oxLDL/ $\beta_2$ GPI/anti- $\beta_2$ GPI complex compared to oxLDL alone, and the upregulated expression of ACAT1, MMP-9 and MCP-1, in addition to the enhanced migration, induced by  $\beta_2$ GPI/anti- $\beta_2$ GPI (Figs. 1D, 2 and 3). However, the present study has limitations. As an intensively investigated member of the TLR family, TLR4 has a critical role in initiating inflammation and participates in VSMC activation (19,21,27,29-31). It has been reported that, different to lipid receptors, TLR4 may potentiate lipid uptake capacity indirectly by activating an inflammatory reaction (29). In the future, the detailed molecular mechanisms, including other potential receptors, including CD36, TLR2 and Fc $\gamma$ , involved in the oxLDL/ $\beta_2$ GPI/anti- $\beta_2$ GPI complex-induced pro-atherogenic pathology process, in addition to the association between oxLDL/ $\beta_2$ GPI/anti- $\beta_2$ GPI complex-induced inflammation and intracellular lipid disorders, should be further determined to clarify the results of the present study. Pro-atherosclerotic switches in VSMC phenotypes is a multi-step and complex mechanism that may be induced by a variety of proinflammatory stimuli (23,24,51). Hence, the effects of the oxLDL/ $\beta_2$ GPI/anti- $\beta_2$ GPI complex on other pro-atherogenic activation methods of VSMCs, including phenotype change, proliferation and apoptosis, require further investigation in order to obtain a full understanding of the function of the oxLDL/ $\beta_2$ GPI/anti- $\beta_2$ GPI complex in the pathology of AS.

In conclusion, the present study demonstrated that the oxLDL/ $\beta_2$ GPI/anti- $\beta_2$ GPI complex was able to induce pro-atherogenic alterations in A7r5 cells, in which the TLR4/NF- $\kappa$ B signaling pathway and ERK1/2 are involved, contributing to the development of atherosclerotic plaque. It strongly suggests that the oxLDL/ $\beta_2$ GPI/anti- $\beta_2$ GPI complex serves a pivotal role in the pro-atherogenic activities of VSMCs and provides an explanation for the clinical observation that the incidence rate of cardiovascular diseases is higher in patients with APS, in addition to a novel research direction and therapy target of AS for patients with autoimmune diseases.

## Acknowledgements

Not applicable.

## Funding

The present study was supported by the National Natural Science Foundation of China (grant no. 81370614) to HZ, the

Youth Fund of Jiangsu Province (grant no. BK20150532) and the Project of Natural Science in Colleges and Universities of Jiangsu Province (grant no. 15KJB310002) to TW.

### Availability of data and material

All data generated or analyzed during this study are included in this published article.

### Authors' contributions

TW and HZ conceived the study and designed the experiments. TW and HO performed the experiments. LX and XW collected and analyzed the experimental results. TW drafted and revised the article.

### Ethics approval and consent to participate

Not applicable.

### Patient consent for publication

Not applicable.

### Competing interests

The authors declare that they have no competing interests.

### References

- Glass CK and Witztum JL: Atherosclerosis. the road ahead. *Cell* 104: 503-516, 2001.
- Amaya-Amaya J, Rojas-Villarraga A and Anaya JM: Cardiovascular disease in the antiphospholipid syndrome. *Lupus* 23: 1288-1291, 2014.
- Matsuura E, Atzeni F, Sarzi-Puttini P, Turiel M, Lopez LR and Nurmohamed MT: Is atherosclerosis an autoimmune disease? *BMC Med* 12: 47, 2014.
- Stern C, Chamley L, Hale L, Kloss M, Speirs A and Baker HW: Antibodies to beta2 glycoprotein I are associated with in vitro fertilization implantation failure as well as recurrent miscarriage: Results of a prevalence study. *Fertil Steril* 70: 938-944, 1998.
- Habe K, Wada H, Matsumoto T, Ohishi K, Ikejiri M, Matsubara K, Morioka T, Kamimoto Y, Ikeda T, Katayama N, *et al*: Presence of antiphospholipid antibody is a risk factor in thrombotic events in patients with antiphospholipid syndrome or relevant diseases. *Intern Med* 97: 345-350, 2013.
- Amory CF, Levine SR, Brey RL, Gebregziabher M, Tuhim S, Tilley BC, Simpson AC, Sacco RL and Mohr JP; APASS-WARSS Collaborators: Antiphospholipid antibodies and recurrent thrombotic events: Persistence and portfolio. *Cerebrovasc Dis* 40: 293-300, 2015.
- Li J, Chi Y, Liu S, Wang L, Han X, Matsuura E and Liu Q: Recombinant domain V of  $\beta_2$ -glycoprotein I inhibits the formation of atherogenic oxLDL/ $\beta_2$ -glycoprotein I complexes. *J Clin Immunol* 34: 669-676, 2014.
- Otomo K, Amengual O, Fujieda Y, Nakagawa H, Kato M, Oku K, Horita T, Yasuda S, Matsumoto M, Nakayama KI, *et al*: Role of apolipoprotein B100 and oxidized low-density lipoprotein in the monocyte tissue factor induction mediated by anti- $\beta_2$  glycoprotein I antibodies. *Lupus* 25: 1288-1298, 2016.
- Ouweneel AB and Van Eck M: Lipoproteins as modulators of atherothrombosis. From endothelial function to primary and secondary coagulation. *Vascul Pharmacol* 82: 1-10, 2016.
- Di Pietro N, Formoso G and Pandolfi A: Physiology and pathophysiology of oxLDL uptake by vascular wall cells in atherosclerosis. *Vascul Pharmacol* 84: 1-7, 2016.
- George J, Harats D, Gilburd B, Afek A, Levy Y, Schneiderman J, Barshack I, Kopolovic J and Shoenfeld Y: Immunolocalization of beta2-glycoprotein I (apolipoprotein H) to human atherosclerotic plaques: Potential implications for lesion progression. *Circulation* 99: 2227-2230, 1999.
- Yu R, Yuan Y, Niu D, Song J, Liu T, Wu J and Wang J: Elevated beta2-glycoprotein I-low-density lipoprotein levels are associated with the presence of diabetic microvascular complications. *J Diabetes Complications* 29: 59-63, 2015.
- Kasahara J, Kobayashi K, Maeshima Y, Yamasaki Y, Yasuda T, Matsuura E and Makino H: Clinical significance of serum oxidized low-density lipoprotein/beta2-glycoprotein I complexes in patients with chronic renal diseases. *Nephron Clin Pract* 98: c15-c24, 2004.
- Lopez D, Garcia-Valladares I, Palafox-Sanchez CA, De La Torre IG, Kobayashi K, Matsuura E and Lopez LR: Oxidized low-density lipoprotein/beta2-glycoprotein I complexes and autoantibodies to oxLig-1/beta2-glycoprotein I in patients with systemic lupus erythematosus and antiphospholipid syndrome. *Am J Clin Pathol* 121: 426-436, 2004.
- Matsuura E and Lopez LR: Are oxidized LDL/beta2-glycoprotein I complexes pathogenic antigens in autoimmune-mediated atherosclerosis? *Clin Dev Immunol* 11: 103-111, 2004.
- Kobayashi K, Kishi M, Atsumi T, Bertolaccini ML, Makino H, Sakairi N, Yamamoto I, Yasuda T, Khamashta MA, Hughes GR, *et al*: Circulating oxidized LDL forms complexes with beta2-glycoprotein I: Implication as an atherogenic auto-antigen. *J Lipid Res* 44: 716-726, 2003.
- Hasunuma Y, Matsuura E, Makita Z, Katahira T, Nishi S and Koike T: Involvement of beta 2-glycoprotein I and anticardiolipin antibodies in oxidatively modified low-density lipoprotein uptake by macrophages. *Clin Exp Immunol* 107: 569-573, 1997.
- Kobayashi K, Tada K, Itabe H, Ueno T, Liu PH, Tsutsumi A, Kuwana M, Yasuda T, Shoenfeld Y, de Groot PG and Matsuura E: Distinguished effects of antiphospholipid antibodies and anti-oxidized LDL antibodies on oxidized LDL uptake by macrophages. *Lupus* 16: 929-938, 2007.
- Xu Y, Kong X, Zhou H, Zhang X, Liu J, Yan J, Xie H and Xie Y: oxLDL/ $\beta_2$ GPI/anti- $\beta_2$ GPI complex induced macrophage differentiation to foam cell involving TLR4/NF-kappa B signal transduction pathway. *Thromb Res* 134: 384-392, 2014.
- Bassi N, Ghirardello A, Iaccarino L, Zampieri S, Rampudda ME, Atzeni F, Sarzi-Puttini P, Shoenfeld Y and Doria A: OxLDL/beta2GPI-anti-oxLDL/beta2GPI complex and atherosclerosis in SLE patients. *Autoimmun Rev* 7: 52-58, 2007.
- Zhang X, Xie Y, Zhou H, Xu Y, Liu J, Xie H and Yan J: Involvement of TLR4 in oxidized LDL/ $\beta_2$ GPI/anti- $\beta_2$ GPI-induced transformation of macrophages to foam cells. *J Atheroscler Thromb* 21: 1140-1151, 2014.
- Tabas I, García-Cardena G and Owens GK: Recent insights into the cellular biology of atherosclerosis. *J Cell Biol* 209: 13-22, 2015.
- Bennett MR, Sinha S and Owens GK: Vascular smooth muscle cells in atherosclerosis. *Circ Res* 118: 692-702, 2016.
- Chistiakov DA, Orekhov AN and Bobryshev YV: Vascular smooth muscle cell in atherosclerosis. *Acta Physiol(Oxf)* 214: 33-50, 2015.
- Hartman J and Frishman WH: Inflammation and atherosclerosis: A review of the role of interleukin-6 in the development of atherosclerosis and the potential for targeted drug therapy. *Cardiol Rev* 22: 147-151, 2014.
- Matsuura E, Lopez LR, Shoenfeld Y and Ames PR:  $\beta_2$ -glycoprotein I and oxidative inflammation in early atherogenesis: A progression from innate to adaptive immunity? *Autoimmun Rev* 12: 241-249, 2012.
- Roshan MH and Tambo A: The role of TLR2, TLR4, and TLR9 in the pathogenesis of atherosclerosis. *Int J Inflam* 2016: 1532832, 2016.
- Hopkins PN: Molecular biology of atherosclerosis. *Physiol Rev* 93: 1317-1542, 2013.
- Yin YW, Liao SQ, Zhang MJ, Liu Y, Li BH, Zhou Y, Chen L, Gao CY, Li JC and Zhang LL: TLR4-mediated inflammation promotes foam cell formation of vascular smooth muscle cell by upregulating ACAT1 expression. *Cell Death Dis* 6: 1659, 2015.
- Yang K, Zhang XJ, Cao LJ, Liu XH, Liu ZH, Wang XQ, Chen QJ, Lu L, Shen WF and Liu Y: Toll-like receptor 4 mediates inflammatory cytokine secretion in smooth muscle cells induced by oxidized low-density lipoprotein. *PLoS One* 9: e95935, 2014.

31. Kong F, Ye B, Cao J, Cai X, Lin L, Huang S, Huang W and Huang Z: Curcumin represses NLRP3 inflammasome activation via TLR4/MyD88/NF- $\kappa$ B and P2X7R signaling in PMA-induced macrophages. *Front Pharmacol* 7: 369, 2016.
32. Jing Q, Xin SM, Cheng ZJ, Zhang WB, Zhang R, Qin YW and Pei G: Activation of p38 mitogen-activated protein kinase by oxidized LDL in vascular smooth muscle cells: Mediation via pertussis toxin-sensitive G proteins and association with oxidized LDL-induced cytotoxicity. *Circ Res* 84: 831-839, 1999.
33. Livak KJ and Schmittgen TD: Analysis of relative gene expression data using real-time quantitative PCR and the 2<sup>-</sup>( $\Delta\Delta C_T$ ) method. *Methods* 25: 402-408, 2001.
34. Newby AC: Matrix metalloproteinases regulate migration, proliferation, and death of vascular smooth muscle cells by degrading matrix and non-matrix substrates. *Cardiovasc Res* 69: 614-624, 2006.
35. Lin J, Kakkar V and Lu X: Impact of MCP-1 in atherosclerosis. *Curr Pharm Des* 20: 4580-4588, 2014.
36. Płóciennikowska A, Hromada-Judycka A, Borzęcka K and Kwiatkowska K: Co-operation of TLR4 and raft proteins in LPS-induced pro-inflammatory signaling. *Cell Mol Life Sci* 72: 557-581, 2015.
37. Ross R and Glomset JA: Atherosclerosis and the arterial smooth muscle cell: Proliferation of smooth muscle is a key event in the genesis of the lesions of atherosclerosis. *Science* 180: 1332-1339, 1973.
38. Badimon L and Vilahur G: Thrombosis formation on atherosclerotic lesions and plaque rupture. *J Intern Med* 276: 618-632, 2014.
39. Sima P, Vannucci L and Vetvicka V: Atherosclerosis as autoimmune disease. *Ann Transl Med* 6: 116, 2018.
40. Tanaka N, Masuoka S, Kusunoki N, Nanki T and Kawai S: Serum resistin level and progression of atherosclerosis during glucocorticoid therapy for systemic autoimmune diseases. *Metabolites* 6: E28, 2016.
41. Rosenfeld ME and Ross R: Macrophage and smooth muscle cell proliferation in atherosclerotic lesions of WHHL and comparably hypercholesterolemic fat-fed rabbits. *Arteriosclerosis* 10: 680-687, 1990.
42. Suckling KE and Strange EF: Role of acyl-CoA: Cholesterol acyltransferase in cellular cholesterol metabolism. *J Lipid Res* 26: 647-671, 1985.
43. Rudel LL, Lee RG and Cockman TL: Acyl coenzyme A: Cholesterol acyltransferase types 1 and 2: Structure and function in atherosclerosis. *Curr Opin Lipidol* 12: 121-127, 2001.
44. Sakashita N, Miyazaki A, Takeya M, Horiuchi S, Chang CC, Chang TY and Takahashi K: Localization of human acyl-coenzyme A: Cholesterol acyltransferase-1 (ACAT-1) in macrophages and in various tissues. *Am J Pathol* 156: 227-236, 2000.
45. Dai Y, Cao Y, Zhang Z, Vallurupalli S and Mehta JL: Xanthine oxidase induces foam cell formation through LOX-1 and NLRP3 activation. *Cardiovasc Drugs Ther* 31: 19-27, 2017.
46. Yang J, Jian R, Yu J, Zhi X, Liao X, Yu J and Zhou P: CD73 regulates vascular smooth muscle cell functions and facilitates atherosclerotic plaque formation. *IUBMB Life* 67: 853-860, 2015.
47. Kim J and Ko J: Human sLZIP promotes atherosclerosis via MMP-9 transcription and vascular smooth muscle cell migration. *FASEB J* 28: 5010-5021, 2014.
48. Chae IG, Yu MH, Im NK, Jung YT, Lee J, Chun KS and Lee IS: Effect of *Rosemarinus officinalis* L. on MMP-9, MCP-1 levels, and cell migration in RAW 264.7 and smooth muscle cells. *J Med Food* 15: 879-886, 2012.
49. Xie HX, Zhou H, Wang HB, Chen DD, Xia LF, Wang T and Yan JC: Anti- $\beta_2$ GPI/ $\beta_2$ GPI induced TF and TNF- $\alpha$  expression in monocytes involving both TLR4/MyD88 and TLR4/TRIF signaling pathways. *Mol Immunol* 53: 246-254, 2013.
50. Cheng YC, Sheen JM, Hu WL and Hung YC: Polyphenols and oxidative stress in atherosclerosis-related ischemic heart disease and stroke. *Oxid Med Cell Longev* 2017: 8526438, 2017.
51. Chaabane C, Coen M and Bochaton-Piallat ML: Smooth muscle cell phenotypic switch: implications for foam cell formation. *Curr Opin Lipidol* 25: 374-379, 2014.



This work is licensed under a Creative Commons Attribution-NonCommercial-NoDerivatives 4.0 International (CC BY-NC-ND 4.0) License.